Title

Phase diagram of URu2–xFexSi2 in high magnetic fields

Journal

Proceedings of the National Academy of Sciences of the United States of America, 114(37)

ISSN

0027-8424

Authors

Ran, Sheng
Jeon, Inho
Pouse, Naveen
et al.

Publication Date

2017-09-12

DOI

10.1073/pnas.1710192114

Peer reviewed

Phase diagram of $URu_{2-x}Fe_xSi_2$ in high magnetic fields

Sheng Ran[a,b], Inho Jeon[b,c], Naveen Pouse[a,b], Alexander J. Breindel[a,b], Noravee Kanchanavatee[a,b,1], Kevin Huang[b,c,2], Andrew Gallagher[d], Kuan-Wen Chen[d], David Graf[d], Ryan E. Baumbach[d], John Singleton[e,f], and M. Brian Maple[a,b,c,3]

[a]Department of Physics, University of California, San Diego, La Jolla, CA 92093; [b]Center for Advanced Nanoscience, University of California, San Diego, La Jolla, CA 92093; [c]Materials Science and Engineering Program, University of California, San Diego, La Jolla, CA 92093; [d]National High Magnetic Field Laboratory, Florida State University, Tallahassee, FL 32313; [e]National High Magnetic Field Laboratory, Los Alamos National Laboratory, Los Alamos, NM 87545; and [f]Department of Physics, The Clarendon Laboratory, University of Oxford, Oxford OX1 2JD, United Kingdom

Contributed by M. Brian Maple, August 1, 2017 (sent for review June 8, 2017); reviewed by Meigan Aronson and Darius H. Torchinsky

Electrical transport measurements were performed on $URu_{2-x}Fe_xSi_2$ single-crystal specimens in high magnetic fields up to 45 T (DC fields) and 60 T (pulsed fields). We observed a systematic evolution of the critical fields for both the hidden-order (HO) and large-moment antiferromagnetic (LMAFM) phases and established the 3D phase diagram of *T*–*H*–*x*. In the HO phase, H/H_0 scales with T/T_0 and collapses onto a single curve. However, in the LMAFM phase, this single scaling relation is not satisfied. Within a certain range of *x* values, the HO phase reenters after the LMAFM phase is suppressed by the magnetic field, similar to the behavior observed for URu_2Si_2 within a certain range of pressures.

hidden order | URu_2Si_2 | high magnetic field | phase diagram

A prime example of emergent behavior in a strongly correlated electron system is the so-called "hidden-order" (HO) phase in the heavy fermion compound URu_2Si_2 that occurs below $T_0 = 17.5$ K and coexists with superconductivity below $T_c = 1.5$ K (1–3). Neutron-scattering experiments reveal the presence of a small antiferromagnetic moment of only 0.03 μ_B/U parallel to the tetragonal *c* axis in the HO phase (4) which is far too small to account for the entropy of $0.2R\ln(2)$ associated with the observed specific heat anomaly (2). Early attempts to identify the order parameter (OP) of the HO phase were unsuccessful, which led to the terminology of hidden order. Over the past three decades, experimentalists and theoreticians alike have expended an enormous amount of effort in trying to identify the OP of the elusive HO phase and many candidates for the HO phase have been proposed (5, 6). However, the nature and origin of the HO phase have not yet been definitively established, although some possibilities have recently emerged (7, 8).

An important aspect of the HO phase is that it exists in close proximity to a large-moment antiferromagnetic (LMAFM) phase that arises for pressures greater than $P_c \geq 0.5$–1.5 GPa (9). Detailed neutron-diffraction experiments suggest that the small antiferromagnetic moment in the HO phase is not intrinsic but is induced by strain that leads to the presence of small regions of the LMAFM phase within the HO phase (10, 11). In addition, inelastic neutron-scattering experiments reveal that at P_c, the spin gap of the incommensurate $Q_1 = (0.4, 0, 0)$ resonance mode related to the heavy quasi-particles increases from 4 meV to 8 meV, while the spin gap of the commensurate $Q_0 = (1, 0, 0)$ resonance mode vanishes (12), demonstrating that the local spin degrees of freedom at Q_0 "freeze out" above P_c and lead to the emergence of the LMAFM phase. This suggests that the HO and LMAFM phases are intimately related and that a detailed understanding of both phases and their competition will be useful in unraveling the nature of the OP of the HO phase.

While experiments under applied pressure provide tantalizing clues regarding the relationship between HO and LMAFM order, progress has been slow due to experimental challenges associated with measurements under such conditions. For example, many methods that are suitable for studying the electronic structure, such as angle-resolved photoemission spectroscopy, scanning tunneling microscopy, quantum oscillations, or high–magnetic-field electrical and thermal transport measurements, are difficult and, in some cases, probably impossible to carry out under high pressure. In recent studies, we demonstrated that tuning URu_2Si_2 by chemical substitution of Fe for Ru affords an opportunity to study the competition between the HO and LMAFM phases at ambient pressure (13–15). Notably, the substitution of the smaller Fe ions for Ru ions in URu_2Si_2 apparently acts as a "chemical pressure" and reproduces the general features of the temperature vs. pressure phase diagram, as demonstrated by electrical resistivity, magnetization, heat capacity, and thermal expansion measurements. We have performed neutron diffraction measurements on single crystalline samples of $URu_{2-x}Fe_xSi_2$, which show that the magnetic moment increases significantly up to $x \approx 0.2$, above which it decreases slowly with *x*, supporting the interpretation that tuning by Fe substitution acts as a chemical pressure (16, 17). Our new results therefore provide a unique opportunity to shed light on the LMAFM phase and its relationship to the elusive HO phase.

Another important method for studying the relationship between HO and LMAFM order is the application of a high magnetic field. Measurements on URu_2Si_2 in high magnetic fields up to 45 T revealed behavior that is consistent with quantum criticality at a field near 37 T, where a cascade of quantum phases occurs at and around the quantum critical point (QCP), suggesting the existence of competing OPs (18, 19). Recent NMR and neutron diffraction experiments have identified the emergent phases with spin density wave (SDW) order (20, 21). By contrast, the substitution of only moderate amounts of Rh for Ru destroys the HO state (22). The associated divergence in

Significance

The mysterious hidden-order (HO) phase in URu_2Si_2 is intimately related to the large-moment antiferromagnetic (LMAFM) phase that is induced under pressure or upon Fe substitution. In this study, we established the 3D phase diagram of transition temperature (*T*)–magnetic field (*H*)–Fe substituent concentration (*x*), which provides ready access to many of the salient features of the HO and LMAFM phases. We observed reentrance of the hidden-order phase after the LMAFM phase is suppressed by the magnetic field and also established a single relation between the transition temperature and the critical magnetic field for the HO phase, which provides constraints on potential models for the order parameter of the HO phase.

Author contributions: S.R. and M.B.M. designed research; S.R., I.J., N.P., A.J.B., N.K., K.H., A.G., K.-W.C., D.G., R.E.B., and J.S. performed research; S.R. analyzed data; and S.R. and M.B.M. wrote the paper.

Reviewers: M.A., Texas A&M University; and D.H.T., Temple University.

The authors declare no conflict of interest.

[1]Present address: Department of Physics, Chulalongkorn University, Pathumwan, 10330, Thailand.

[2]Present address: National High Magnetic Field Laboratory, Florida State University, Tallahassee, FL 32313.

[3]To whom correspondence should be addressed. Email: mbmaple@ucsd.edu.

the density of electronic states and a much simpler phase diagram are observed in high magnetic fields. High–magnetic-field experiments have also been performed on URu_2Si_2 under pressure and yielded some controversial results. An early experiment, carried out under pressures of up to 1.1 GPa, showed that development of the LMAFM phase did not alter significantly the temperature (T)–magnetic field (H) phase diagram of URu_2Si_2, suggesting adiabatic continuity between the HO and LMAFM phases (23). Subsequent experiments, with pressures up to 1.9 GPa, showed that the HO and LMAFM phase boundaries have different curvatures and that the HO phase reenters when the LMAFM phase is suppressed by a magnetic field (24).

Given that Fe substitution provides an alternative route for accessing both the HO and LMAFM phases, the performance of transport, magnetic, or thermal measurements at high magnetic fields as a function of Fe concentration x is expected to reveal important insights into the LMAFM phase and its relationship with the HO phase. In this study, we carried out electrical transport measurements on $URu_{2-x}Fe_xSi_2$ single crystals in high magnetic fields of up to 45 T in the hybrid magnet and 60 T in the pulsed-field magnet to investigate the T–H phase diagram of the $URu_{2-x}Fe_xSi_2$ system. We observed a systematic evolution of the critical fields for both the HO and LMAFM phases and established the 3D T–H–x phase diagram. For $x = 0.15$ and 0.2, we observed the reentrance of the HO phase upon suppression of the LMAFM phase.

Results

Electrical resistivity measurements were performed as a function of magnetic field at various temperatures on nine different $URu_{2-x}Fe_xSi_2$ single-crystalline samples with Fe concentrations x ranging from 0 to 0.3, to examine both the HO and LMAFM phases. The data collected in the dc-field hybrid magnet are presented in Fig. 1. The data collected in pulsed-field magnets are fully consistent with these results. Features associated with different phase transitions are apparent, which are further illustrated in Fig. 2 with ($x = 0$, $T = 0.38$ K) and ($x = 0.15$, $T = 5$ K) as two examples. Previous studies show that the HO phase transition in URu_2Si_2 is suppressed to zero temperature near 35 T (18, 19). This is manifested in the ($x = 0$, $T = 0.38$ K) data as a sharp increase in resistance. Upon further increase of the magnetic field, a cascade of quantum phases was previously observed. One of these phases has very robust features in the resistance data and has recently been identified with SDW order (20, 21). For ($x = 0$, $T = 0.38$ K), the boundary of this phase is indicated with red arrows in Fig. 2*A*. We did not observe the subtle features associated with the two other phases in the vicinity of the magnetic field where the HO is suppressed. On the other hand, there are subtle features in the field range of 20–30 T, which can be seen more clearly in the derivative dR/dH. These features evolve consistently with increasing temperature and Fe concentration and therefore may indicate the boundary of another phase. To illustrate this, we show the color contour plot of the resistance value for $x = 0$ as a function of magnetic field and temperature in

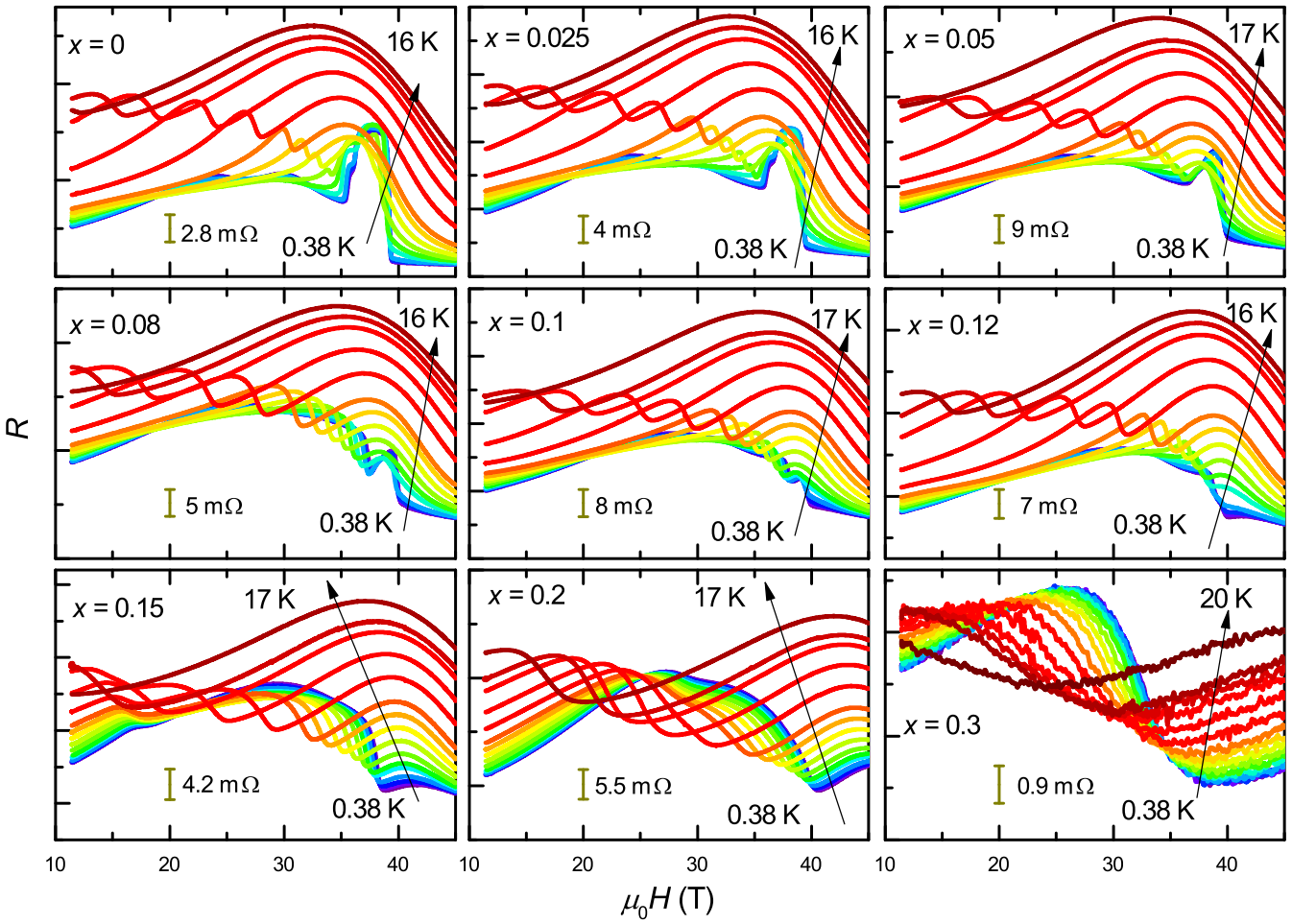

Fig. 1. Electrical resistance R vs. magnetic field H at different temperatures for $URu_{2-x}Fe_xSi_2$ single crystals, with $x = 0$, 0.025, 0.05, 0.08, 0.1, 0.12, 0.15, 0.2, and 0.3. The magnetic field was applied along the c axis. Bars on each graph represent 10% of the maximum value on the resistance axis.

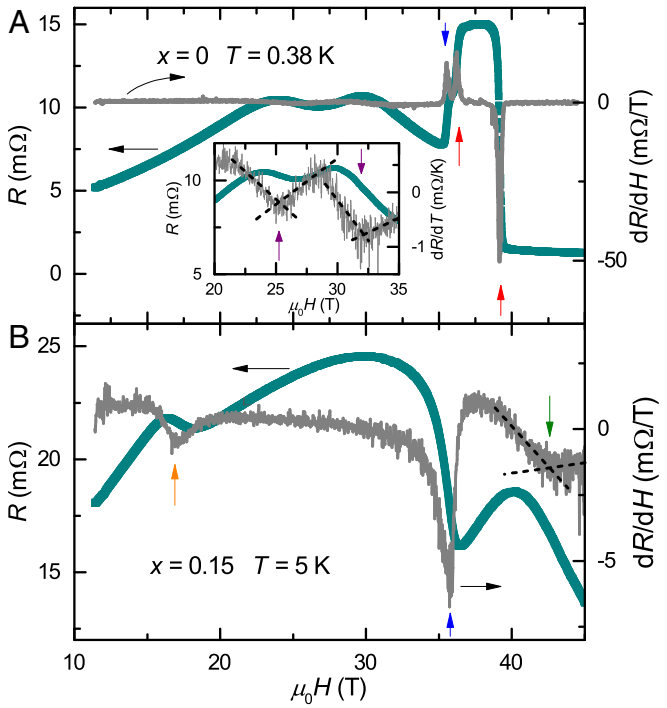

Fig. 2. Electrical resistance R and its derivative dR/dH vs. magnetic field H for (*A*) $x = 0$, $T = 0.38$ K and (*B*) $x = 0.15$, $T = 5$ K. The magnetic field was applied along the c axis. Arrows indicate the fields for phase transitions or crossovers.

Fig. 3. A clear contrast representing a change in electrical resistance is seen, which seems to define the boundary of a new phase. Similar results were reported previously in resistance, quantum oscillation, and NMR measurements (20, 25, 26), indicating a possible phase transition well within the HO phase.

At 5 K, the $x = 0.15$ sample is in the LMAFM phase in low magnetic field. A field of roughly 17 T drives it into a different phase, evidenced by a peak in resistance. Similar results were reported for URu_2Si_2 under applied pressure (24). URu_2Si_2 is in the LMAFM phase under pressure above $P_c \geq 0.5$–1.5 GPa. Thermal expansion measurements reveal that in a magnetic field the LMAFM phase is suppressed and another phase is induced (24). Inelastic neutron-scattering measurements further show that the spin gap at the commensurate $Q_0 = (1, 0, 0)$ resonance mode, which is characteristic of the HO phase, reappears in the induced phase and therefore demonstrates the reentrance of the HO phase in the magnetic field (24). Given that Fe substitution acts as a chemical pressure and reproduces the applied pressure phase diagram in zero magnetic field, it is very likely that the phase transition observed here is also the reentrance of the HO phase. In this paper, we label the field-induced phase occurring after the LMAFM phase as HO*. The terminology "reentrance" is usually applied to a situation in which the continuous change of a control parameter causes a given symmetry-breaking phase to transform into a different symmetry-breaking phase after which it then "reenters" the original symmetry-breaking phase. In the present work, two control parameters are concurrently used to achieve reentrance: magnetic field and chemical substitution.

A further increase of the magnetic field to about 37 T suppresses the HO phase as indicated by another drop in resistance. In even higher magnetic field, there is a field-induced recovery of the normal metallic phase, with some or all of the magnetic moments of the f electrons aligned by H (19), which is manifested as a change of slope in the derivative of the resistance. The broad maximum in resistance is also tracked as a function of temperature for all of the samples below $x = 0.3$. A similar resistivity maximum occurs in other systems with itinerant metamagnetic transitions, such as $Sr_3Ru_2O_7$, $CeRu_2Si_2$, and UPt_3 (27–29), and has been used as an experimental protocol for itinerant electron metamagnetic quantum-phase transitions.

Having established the criteria for identifying different phase transitions, we can map out the temperature–magnetic-field phase diagrams for different Fe concentrations, which are presented in Fig. 4. Based on these phase diagrams, we can further construct a 3D phase diagram with temperature T, magnetic field H, and Fe concentration x as the three axes, as shown in Fig. 5. We find that the combination of magnetic field and Fe substitution provides ready access to the salient ground states of $URu_{2-x}Fe_xSi_2$: the HO, LMAFM, and SDW phases; field-induced recovery of the normal metallic phase (labeled FL in Fig. 5); and broad maximum in resistance; as well as the possible new phase in low fields (labeled P1 in Fig. 5). In addition, the 3D phase diagram shows a very smooth, continuous surface extending from the HO phase to the HO* phase. This is consistent with our hypothesis that the HO* phase is the reentrance of the HO phase. Future experiments, such as inelastic neutron scattering and magnetization measurements, are required to investigate the nature of the HO* phase.

Both the HO and LMAFM phases are tuned systematically by varying the magnetic field. In Fig. 6, we plot the magnetic field needed to suppress the HO and LMAFM phases, H_0, as a function of Fe substituent concentration (bottom axis). The H_0 for the HO phase increases from 35 T for $x = 0$ to about 38 T for $x = 0.12$ in a linear manner. The H_0 for the LMAFM phase increases a lot faster, from 16.7 T for $x = 0.15$ to 33 T for $x = 0.3$. For comparison, we also plot H_0 as a function of applied pressure (24) (top axis), with a conversion of $\Delta x/\Delta P = 0.1$ GPa^{-1} that has been reported previously (13, 14). The two sets of data match quite well in the HO range. On the other hand, the LMAFM phase was observed under pressures that are equivalent to rather low Fe concentration; however, we did not observe the LMAFM phase for $x < 0.12$.

For $x = 0.12$, other experiments indicate the sample is in the LMAFM phase in zero magnetic field (15, 16). By extrapolating the value of H_0 of the LMAFM to $x = 0.12$, we obtain a value

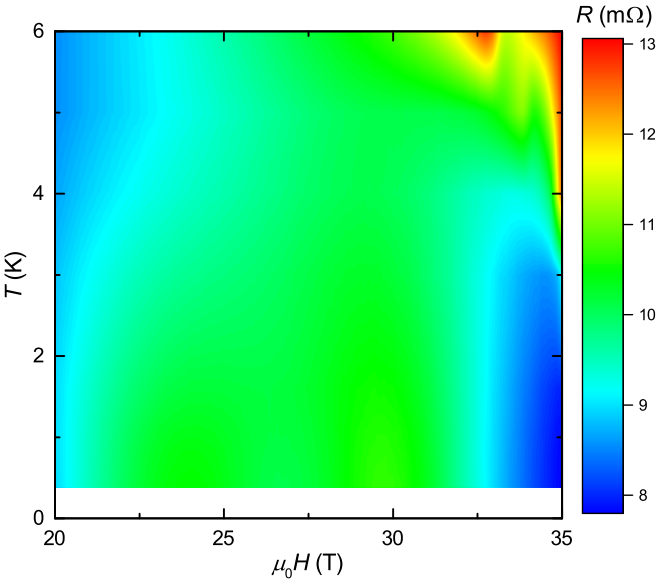

Fig. 3. Color contour plot of the magnitude of the resistance for $x = 0$ as a function of magnetic field H and temperature T. The contrast in color reflecting the change in magnitude of the resistance appears to delineate the boundary of a new phase.

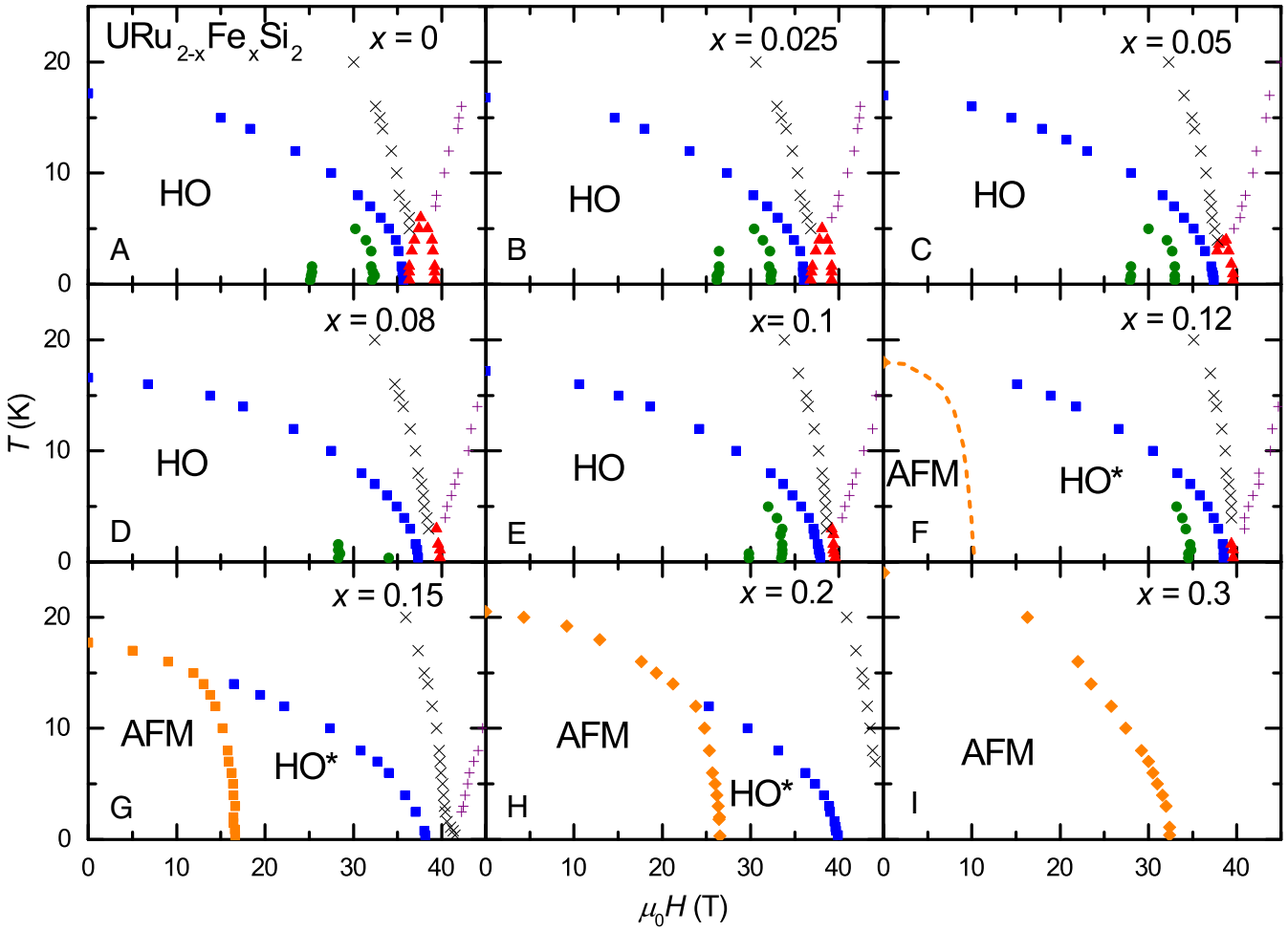

Fig. 4. (*A–I*) Temperature (T)–magnetic-field (H) phase diagrams for $URu_{2-x}Fe_xSi_2$ single crystals, with $x = 0$ (*A*), 0.025 (*B*), 0.05 (*C*), 0.08 (*D*), 0.1 (*E*), 0.12 (*F*), 0.15 (*G*), 0.2 (*H*), and 0.3 (*I*). The magnetic field was applied along the *c* axis. The symbols have the following meaning: blue squares, HO and HO* phase transitions; orange diamonds, LMAFM phase transitions; green circles, possible phase transitions in low field; red triangles, SDW phase; black crosses, broad maximum in the resistance; and purple plus sign, crossover to normal metallic phase.

of H_0 less than 10 T. In the fields above 10 T, the sample is in the HO phase. However, we did not observe a signature of the phase transition from the LMAFM to the HO phase. This may be consistent with the scenario of adiabatic continuity between the HO and LMAFM phases reported previously under 1.1 GPa (23), given that $x = 0.12$ converts to a similar chemical pressure (13–15).

Fig. 7 presents another comparison between the HO and LMAFM phases. Even though H_0 for the HO phase increases with x, H/H_0 scales with T/T_0 very well and collapses onto a single curve. This again supports our hypothesis that the HO* phase is the reentrance of the HO phase. This single scaling leads to unified critical behavior for the HO phase, $T \propto (H_0-H)^{\alpha}$, with $\alpha = 0.51$ (fit is performed in the range of $0.9H_0$ to H_0). On the other hand, the LMAFM phase does not exhibit a single scaling. The fit of $T \propto (H_0-H)^{\alpha}$ to the data in the LMAFM phase yields $\alpha = 0.55$, 0.53, and 0.51 for $x = 0.15$, 0.2, and 0.3. Mean-field theory also predicts that both the transition temperature as a function of H and the critical field as a function of T intersect the axes in a perpendicular manner and both can be expanded in a series of even powers of H and T (30, 31). A plot of $(H/H_0)^2$ vs. $(T/T_0)^2$ should therefore yield a line that intersects both axes in an approximately linear fashion, as shown in a previous study (18). The fit of the equation $(T/T_0)^n + (H/H_0)^n = 1$ to our data in the HO phase yields $n = 1.8$. This is demonstrated by the linear variation of $(T/T_0)^{1.8}$ with $(H/H_0)^{1.8}$ shown in Fig. 7, *Inset*. The same equation does not work well in the LMAFM region. These results put strong constraints on the potential theoretical model for the OP of the HO phase.

After the HO phase is suppressed, a phase recently identified with SDW order emerges (20, 21). This phase is labeled P1 on the 3D phase diagram in Fig. 5. Note that we did not observe this phase for samples above $x = 0.12$, even though the HO phase reenters at high magnetic field, indicating the HO phase is not a necessary condition for the appearance of the SDW.

The upper field boundary of the SDW seems to remain constant, at about 40 T, while the lower boundary is gradually interrupted by the HO phase, as the Fe concentration increases. This suggests that the order parameters of the HO and LMAFM phases compete and Fe substitution seems to favor the HO. It has been suggested that the broad maximum in the magnetoresistance in the range of 30–40 T is the precursor of magnetic ordering (19). This maximum narrows and systematically shifts to higher fields as the temperature is reduced and indeed extrapolates to a critical-field H_m within the range of the SDW for $x \leq 0.12$. The exact location of H_m can be obtained by fitting the data with a similar power-law scaling as done for the HO phase, $T \sim (H_m-H)^{\beta}$. The results are presented in Fig. 8. For $x = 0.15$, H_m deviates from this behavior and increases faster as the temperature is reduced below 2.5 K, as shown in Fig. 4*G*.

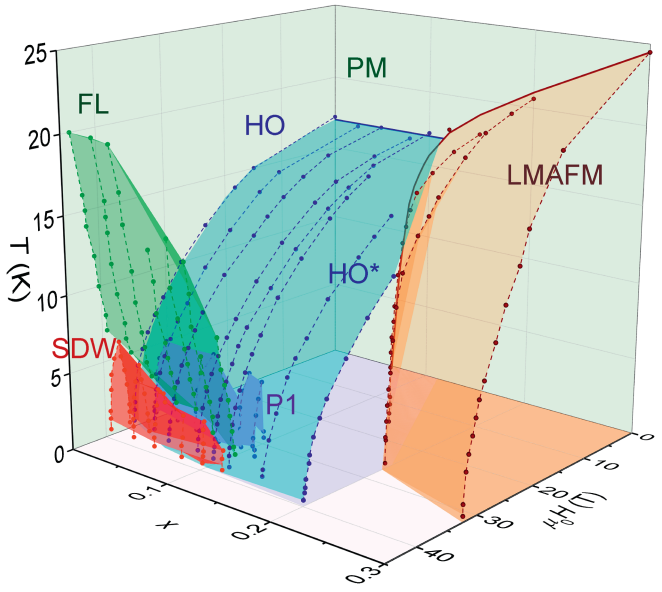

Fig. 5. Three-dimensional phase diagram for $URu_{2-x}Fe_xSi_2$ single crystals, with temperature T, magnetic field H, and Fe concentration x as the three axes. The magnetic field was applied along the c axis. The labels have the following meaning: HO, hidden-order phase; HO*, reentrant HO phase; LMAFM, large-moment antiferromagnetic phase; SDW, spin density wave; FL, field-induced recovery of the normal metallic phase; P1, possible new phase in low fields; and PM, paramagnetic phase at high temperature.

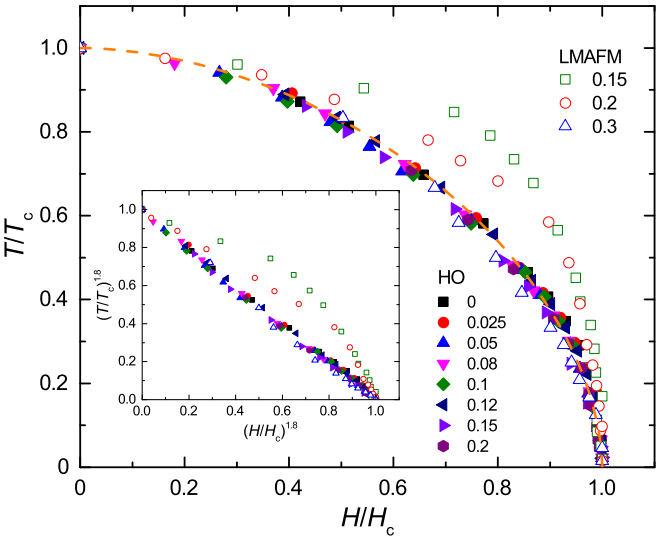

Fig. 7. Normalized critical-field H/H_0 as a function of normalized critical temperature T/T_0 for $URu_{2-x}Fe_xSi_2$ single crystals, with $x = 0$, 0.025, 0.05, 0.08, 0.1, 0.12, 0.15, 0.2, and 0.3. The solid and open symbols represent data for the HO and LMAFM phases, respectively. The dashed line represents the best fit of the equation $(T/T_0)^n + (H/H_0)^n = 1$ to the data, which yields $n = 1.8$. *Inset* shows $(T/T_0)^{1.8}$ as a function of $(H/H_0)^{1.8}$ for the samples.

Extrapolation of the data above 2.5 K leads to $H_m = 40.4$ T, which exceeds the upper-field boundary of the SDW. This is likely the reason why the SDW is not induced for $x = 0.15$ and above. It will be interesting to conduct future measurements to determine the exact nature of the phase below 2.5 K and compare it to that of the SDW.

Figs. 2*A*, *Inset* and 3 indicate a possible phase transition that lies well within the HO phase in the field range 20–30 T, which is also labeled P1 in Fig. 5. Previous Hall resistivity and quantum oscillation measurements reveal similar results in the parent compound URu_2Si_2 (25). A novel quantum oscillation appears above this phase transition, indicating that it is likely associated with the abrupt reconstruction of the Fermi surface (25). The driving force for the Fermi surface reconstruction is still unclear. Fe substitution provides systematic tuning of this possible phase transition and a good opportunity to study it in detail in future experiments. In particular, our experiments show that this Fermi surface reconstruction does not occur in the LMAFM phase or the HO phase when it reenters.

Concluding Remarks

We performed electrical transport measurements on $URu_{2-x}Fe_xSi_2$ single crystals in high magnetic fields up to 45 T,

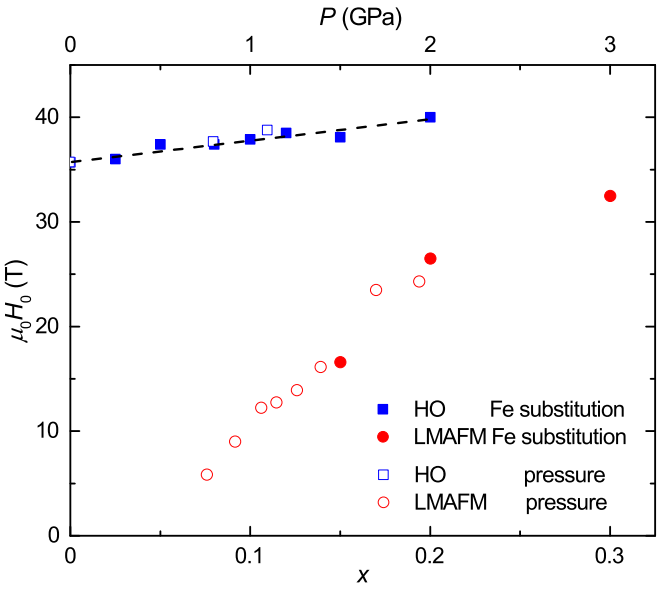

Fig. 6. Critical-field H_0 as a function of Fe concentration x (bottom axis) and applied pressure P (top axis) (24).

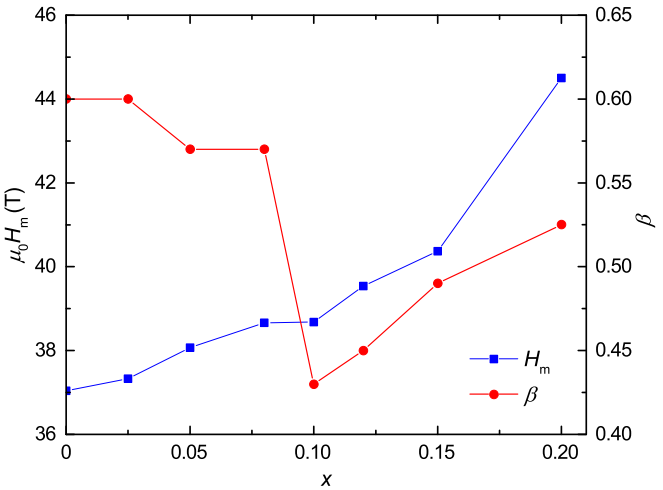

Fig. 8. Extrapolated critical field of the broad maximum in the magnetoresistance H_m and power-law scaling exponent β vs. Fe substituent concentration x. The power-law scaling function used for this procedure has the form $T \propto (H_m - H)^{\beta}$.

using the 35-T dc and 45-T hybrid dc magnets at the National High Magnetic Field Laboratory (NHMFL), Tallahassee, FL, and 60 T using the 60-T pulsed-field magnet at the NHMFL, Los Alamos, NM, to investigate the temperature–magnetic-field phase diagram of the $URu_{2-x}Fe_xSi_2$ system. We observed a systematic evolution of the critical fields for both the HO and LMAFM phases and established a 3D phase diagram of T–H–x. For the HO phase H/H_0 scales with T/T_0 quite well and collapses onto a single curve. In contrast, the LMAFM phase does not follow a single scaling curve. The HO phase reenters after the LMAFM phase is suppressed, similar to what was observed under pressure.

Materials and Methods

Single crystals of Fe-substituted URu_2Si_2 were grown by the Czochralski method in a tetra-arc furnace, as reported previously (15). The quality of the samples was determined by Laue X-ray diffraction patterns together with X-ray powder diffraction measurements. Electrical resistivity measurements were performed at the NHMFL, Tallahassee, using the 35-T dc and 45-T hybrid dc magnets, and at the NHMFL, Los Alamos, using the 60-T pulsed-field magnet. Great care was taken to ensure that the value of the resistance was independent of current, showing that sample heating was negligible.

ACKNOWLEDGMENTS. Research at University of California, San Diego was supported by the US Department of Energy (DOE) Basic Energy Sciences under Grant DE-FG02-04ER46105 (materials synthesis and characterization), the US National Science Foundation (NSF) under Grant DMR-1206553 (low-temperature measurements), and the National Nuclear Security Administration under the Stewardship Science Academic Alliance Program through the US DOE under Grant DE-NA0002909 (high–magnetic-field measurements). Research at the National High Magnetic Field Laboratory (NHMFL) was supported by NSF Cooperative Agreement DMR-1157490, the State of Florida, and the DOE. A portion of this work was supported by the NHMFL User Collaboration Grant Program.

1. Palstra TTM, et al. (1985) Superconducting and magnetic transitions in the heavy-fermion system uranium ruthenium silicide (URu_2Si_2). *Phys Rev Lett* 55:2727–2730.
2. Maple MB, et al. (1986) Partially gapped Fermi surface in the heavy-electron superconductor uranium ruthenium silicide (URu_2Si_2). *Phys Rev Lett* 56:185–188.
3. Schlabitz W, et al. (1986) Superconductivity and magnetic order in a strongly interacting Fermi-system: Uranium ruthenium silicide (URu_2Si_2). *Z Phys B Condens Matter* 62:171–177.
4. Broholm C, et al. (1987) Magnetic excitations and ordering in the heavy-electron superconductor uranium ruthenium silicide (URu_2Si_2). *Phys Rev Lett* 58:1467–1470.
5. Mydosh JA, Oppeneer PM (2011) Colloquium: Hidden order, superconductivity, and magnetism: The unsolved case of URu_2Si_2. *Rev Mod Phys* 83:1301–1322.
6. Mydosh J, Oppeneer P (2014) Hidden order behaviour in URu_2Si_2. *Philos Mag* 94:3642–3662.
7. Kung HH, et al. (2015) Chirality density wave of the "hidden order" phase in URu_2Si_2. *Science* 347:1339–1342.
8. Kung HH, et al. (2016) Analogy between the "hidden order" and the orbital antiferromagnetism in $URu_{2-x}Fe_xSi_2$. *Phys Rev Lett* 117:227601.
9. Butch NP, et al. (2010) Antiferromagnetic critical pressure in URu_2Si_2 under hydrostatic conditions. *Phys Rev B* 82:060408.
10. Amitsuka H, et al. (2007) Pressure-temperature phase diagram of the heavy-electron superconductor URu_2Si_2. *J Magn Magn Mater* 310:214–220.
11. Niklowitz PG, et al. (2010) Parasitic small-moment antiferromagnetism and nonlinear coupling of hidden order and antiferromagnetism in URu_2Si_2 observed by larmor diffraction. *Phys Rev Lett* 104:106406.
12. Bourdarot F, et al. (2010) Precise study of the resonance at Q_0 = (1,0,0) in URu_2Si_2. *J Phys Soc Jpn* 79:064719.
13. Kanchanavatee N, et al. (2011) Twofold enhancement of the hidden-order/large-moment antiferromagnetic phase boundary in the $URu_{2-x}Fe_xSi_2$ system. *Phys Rev B* 84:245122.
14. Wolowiec CT, Kanchanavatee N, Huang K, Ran S, Maple MB (2016) Evolution of critical pressure with increasing Fe substitution in the heavy-fermion system $URu_{2-x}Fe_xSi_2$. *Phys Rev B* 94:085145.
15. Ran S, et al. (2016) Phase diagram and thermal expansion measurements on the system $URu_{2-x}Fe_xSi_2$. *Proc Natl Acad Sci USA* 113:13348–13353.
16. Das P, et al. (2015) Chemical pressure tuning of URu_2Si_2 via isoelectronic substitution of Ru with Fe. *Phys Rev B* 91:085122.
17. Butch NP, et al. (2016) Distinct magnetic spectra in the hidden order and antiferromagnetic phases in $URu_{2-x}Fe_xSi_2$. *Phys Rev B* 94:201102.
18. Harrison N, Jaime M, Mydosh JA (2003) Reentrant hidden order at a metamagnetic quantum critical end point. *Phys Rev Lett* 90:096402.
19. Kim KH, Harrison N, Jaime M, Boebinger GS, Mydosh JA (2003) Magnetic-field-induced quantum critical point and competing order parameters in URu_2Si_2. *Phys Rev Lett* 91:256401.
20. Sakai H, et al. (2014) Emergent antiferromagnetism out of the "hidden-order" state in URu_2Si_2: High magnetic field nuclear magnetic resonance to 40 T. *Phys Rev Lett* 112:236401.
21. Knafo W, et al. (2016) Field-induced spin-density wave beyond hidden order in URu_2Si_2. *Nat Commun* 7:13075.
22. Silhanek AV, et al. (2005) Quantum critical 5*f* electrons avoid singularities in $U(Ru,Rh)_2Si_2$. *Phys Rev Lett* 95:026403.
23. Jo YJ, et al. (2007) Field-induced fermi surface reconstruction and adiabatic continuity between antiferromagnetism and the hidden-order state in URu_2Si_2. *Phys Rev Lett* 98:166404.
24. Aoki D, et al. (2009) Field reentrance of the hidden order state of URu_2Si_2 under pressure. *J Phys Soc Jpn* 78:053701.
25. Shishido H, et al. (2009) Possible phase transition deep inside the hidden order phase of URu_2Si_2. *Phys Rev Lett* 102:156403.
26. Scheerer GW, Knafo W, Aoki D, Flouquet J (2012) Angular dependence of the high-magnetic-field phase diagram of URu_2Si_2. *J Phys Soc Jpn* 81:SB005.
27. Grigera SA, et al. (2001) Magnetic field-tuned quantum criticality in the metallic ruthenate $Sr_3Ru_2O_7$. *Science* 294:329–332.
28. Kambe S, Suderow H, Flouquet J, Haen P, Lejay P (1995) Field-induced renormalization observed by magnetoresistance in $CeRu_2Si_2$. *Solid State Commun* 95:449–453.
29. Kim JS, Hall D, Heuser K, Stewart GR (2000) Indications of non-Fermi liquid behavior at the metamagnetic transition of UPt_3. *Solid State Commun* 114:413–418.
30. Dieterich W, Fulde P (1973) Magnetic field dependence of the Peierls instability in one-dimensional conductors. *Z Phy A Hadrons Nucl* 265:239–243.
31. Harrison N (1999) Destabilization of a charge-density wave by an oscillatory chemical potential. *Phys Rev Lett* 83:1395–1398.